AWARD NUMBER: W81XWH-16-1-0376

TITLE: SERS Nanosensors for in vivo Glucose Sensing

PRINCIPAL INVESTIGATOR: Milan Mrksich

CONTRACTING ORGANIZATION: Northwestern University
Chicago, IL 60611

REPORT DATE: Sept 2019

TYPE OF REPORT: Annual Report

PREPARED FOR: U.S. Army Medical Research and Materiel Command
Fort Detrick, Maryland 21702-5012

REPORT DOCUMENTATION PAGE

Form Approved
OMB No. 0704-0188

1. REPORT DATE	2. REPORT TYPE	3. DATES COVERED
SEPTEMBER 2019	Annual report	1 Sep 2018- 31 Aug 2019

4. TITLE AND SUBTITLE

SERS Nanosensors for in vivo Glucose Sensing

5a. CONTRACT NUMBER
W81XWH-16-1-0376

5b. GRANT NUMBER

5c. PROGRAM ELEMENT NUMBER

6. AUTHOR(S)

Milan Mrksich, Ji Eun Park, Vitor Brasiliense, Ju-Young Kim, Eric Berns, Pradeep Bugga,
E-Mail: milan.mrksich@northwestern.edu

5d. PROJECT NUMBER

5e. TASK NUMBER

5f. WORK UNIT NUMBER

7. PERFORMING ORGANIZATION NAME(S) AND ADDRESS(ES)

Northwestern University
Evanston, Illinois 60208

8. PERFORMING ORGANIZATION REPORT NUMBER

9. SPONSORING / MONITORING AGENCY NAME(S) AND ADDRESS(ES)

U.S. Army Medical Research and Materiel Command
Fort Detrick, Maryland 21702-5012

10. SPONSOR/MONITOR'S ACRONYM(S)

11. SPONSOR/MONITOR'S REPORT NUMBER(S)

12. DISTRIBUTION / AVAILABILITY STATEMENT

Approved for Public Release; Distribution Unlimited

13. SUPPLEMENTARY NOTES

14. ABSTRACT

The goal of this program is to develop small and sensitive nanosensors for the continuous glucose monitoring in living tissue without the need for drawing blood. A major advantage of the transdermal sensors we are developing is to directly detect glucose itself – not the byproducts of its transformation. The technique we use – surface-enhanced Raman spectroscopy (SERS) – is based on light and informs on the presence of glucose on or near metallic nanosensors. **In Year 1**, we have worked on the development of i) sensitive nanosensors, ii) selective capture layers that can be immobilized onto metal surfaces, and iii) the integration of both. We have successfully developed a novel SERS nanoplatform that integrates gold nanorods with biocompatible hydrogels of variable stiffness. **In Year 2**, we have implemented the glucose-capture ligand on the gold nanorod surface that are already integrated with polymeric microneedle patches. The stability of the nanorods in buffer conditions as well as organic solvents was evaluated. Additionally, SERS activity and device performance after functionalizing the surface with a pH-sensitive Raman reporter molecule was investigated by measuring reversible pH change from solution and in a skin phantom. **In Year 3**, the SERS performance of the plasmonic microneedle was evaluated *ex vivo* (human skin). In addition to this platform, we successfully fabricated an electrochemical microneedle sensor with SERS activity that allows us to apply potential and detect analytes using SERS without the need of a capture ligand. We have demonstrated the sensing capability of this sensor platform by detecting model molecules (benzenethiol, caffeine, and theobromine).

In addition, we developed an electrochemical strategy to reversibly localize analytes within the SERS detecting zone and enable separation of SERS signals from different analytes through multivariate analysis.					
15. SUBJECT TERMS Glucose, sensing, boronic acid, SERS, spectroscopy, hydrogel, microneedle array, continuous glucose monitoring, medical device					
16. SECURITY CLASSIFICATION OF:			**17. LIMITATION OF ABSTRACT**	**18. NUMBER OF PAGES**	**19a. NAME OF RESPONSIBLE PERSON** USAMRMC
a. REPORT Unclassified	**b. ABSTRACT** Unclassified	**c. THIS PAGE** Unclassified	Unclassified	28	**19b. TELEPHONE NUMBER** *(include area code)*

Standard Form 298 (Rev. 8-98)
Prescribed by ANSI Std. Z39.18

Table of Contents

Page

1. INTRODUCTION

Diabetes is a chronic disease in which levels of blood glucose – a small molecule that serves as an energy source – exceed the norm and pose a host of primary and secondary health complications. The goal of this program is to lighten the physical and psychological burden that daily blood glucose checks represent for patients and to improve their long-term health through the development of small and sensitive nanosensors that *continuously* detect and measure glucose in living tissue over a long period of time (several months) without the need for drawing blood. A major advantage of the transdermal sensors we are developing is to *directly* detect glucose itself – not the byproducts of glucose transformation - which require external reagents that add extra costs and steps, and which can respond to other molecules in the blood, such as fructose, leading to false inflation of measurements.

2. KEYWORDS

Glucose, diabetes, pH, biosensing, SERS, Raman scattering, spectroscopy, microneedle array, plasmonic microneedles, transdermal patch, continuous monitoring, ex vivo, electrochemical sensing, reversible

3. ACCOMPLISHMENTS

Major goals of the project
As stated in the approved Statement of Work (SOW), the major goals of Year 3 of this program were:

1- **Implant nanosensors with SERS/SESORS detection** led by Site 1 (Van Duyne lab and Mrksich labs).
We set up a home-built microscope with surface-enhanced spatially-offset Raman spectroscopy (SESORS) capability. We have optimized the set up for the maximum power and demonstrated its SORS ability by detecting a sub-layer.
2- **In vivo glucose sensing in small animals (rats) for 3 months** carried out by both Site 1 and 2 (Van Duyne and Mrksich labs).
Preliminary experiments in skin using plasmonic microneedle array was performed in rat skin, pig skin, and in human skin. We successfully demonstrated the sensing ability of the plasmonic microneedle array by detecting skin pH while inserted in human skin. Lastly, for the electrochemical microneedle sensor, we applied potential while inserted in human skin.
3- **Functional nanosensors for the detection of glucose by SERS/SESORS through skin** carried out by both Sites 1 and 2 (Van Duyne and Mrksich labs).
Due to difficulty in synthesizing glucose capture ligands with effective binding, we have explored alternative strategies to reversibly adsorb analytes to the surface using electrochemical methods. We demonstrated the applied potential can be used to modulate the surface chemistry (and therefore analyte binding constant), enabling selective sensing. This method also enables application of interpretable multivariate analysis, which has the potential of coping with presence of interfering biomolecules (which are likely to be present in vivo).

1- SESORS set up

We proposed to use surface-enhanced spatially-offset Raman spectroscopy (SESORS) to detect analytes through skin while a SERS sensor is inserted in skin. In order to do this, we have built the SESORS set up with a home-built microscope where we can change the focusing and collection objective lens to perform spatially-offset measurements (Setup 1). We used a 785-nm diode laser and the set up was optimized so that the output power was the maximum.

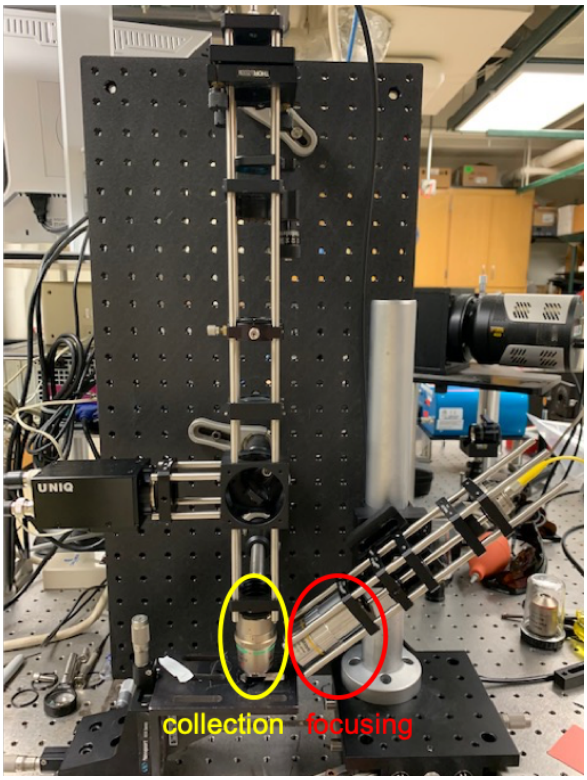

Setup 1. Image of the home-built SESORS set up. Home-built microscope set up with a 785-nm diode laser and a capability to change the focusing (circled with red) and collection (circled with yellow) objective lens position for spatially-offset measurement. Objectives inserted are 10x for focusing and 20x ELWD for collecting.

2- Plasmonic microneedle arrays for transdermal SERS sensor platform

During the second year, we successfully fabricated a plasmonic microneedle arrays sensor and evaluated the sensor platform functionality by detecting a biologically important metric, pH. For the third year, we focused on characterizing the plasmonic microneedle arrays sensor for detecting pH *in situ* and *ex vivo*, as well as its mechanical stability. Our sensor was the first to combine SERS-active nanoparticles with polymeric microneedle arrays and demonstrated both *in situ* and *ex vivo* sensing. We note that this work was published in Nano Letters (*Nano Letters,* **2019***, 19,* 6862-6868) .

2.1 Summary of the overall sensor design/fabrication

Combining the sensing capability of SERS with microneedle arrays creates an opportunity to detect biomolecules *in situ* through tissue or skin that are otherwise difficult to detect in a relatively non-invasive fashion. Microneedle arrays have received attention as a painless and minimally-invasive sensor platform for monitoring analytes in biofluids, especially in the interstitial fluid (ISF).[1–6] Here, we integrated SERS with polymeric microneedle arrays as a minimally invasive, innovative platform for biomolecule sensing, with particular vision towards detecting glucose in the ISF.

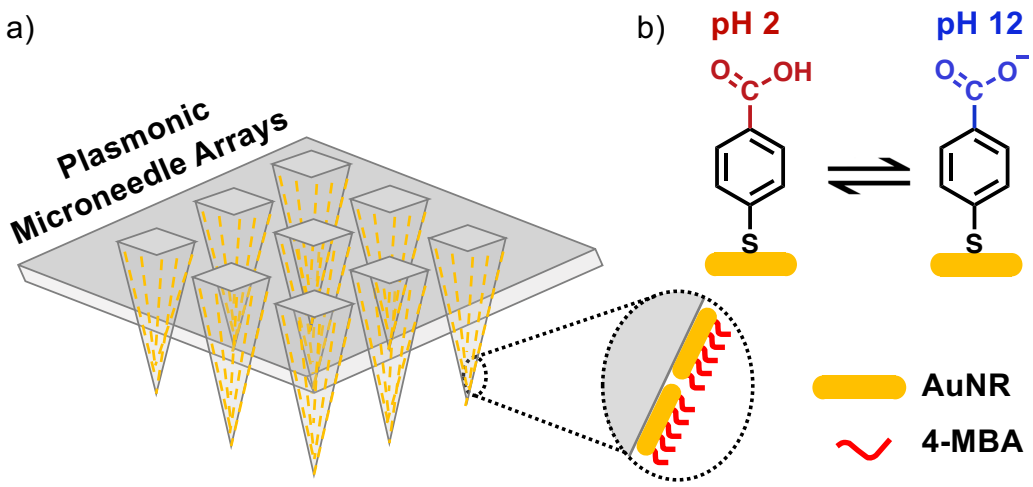

Figure 1. Plasmonic microneedle arrays sensor design. a) Gold nanorods (AuNRs) functionalized with a pH-sensitive molecule 4-mercaptobenzoic acid (4-MBA) are decorated on the surface of NOA microneedle arrays. b) pH-sensitive 4-MBA can be protonated at pH 2 and deprotonated at pH 12.

For the polymer, we chose commercially-available Norland Optical Adhesive (NOA) 65 that is known to be optically transparent at 785 nm, which is critical since it allows Raman scattered light to be detected through the microneedle arrays and thus enables *in situ* sensing. Although the exact composition of NOA 65 is protected by a commercial patent, the polymer consists of mercaptoester functional groups. We hypothesized that the functional group would allow us to functionalize SERS-active nanoparticles such as AuNRs onto the polymer surface. Lastly, the biocompatibility of various NOAs have been demonstrated in literature by using NOA as a cell culture scaffold for endothelial cells[7], fibroblasts[8], HeLa cells and neurons[9], and human embryonic stem cells[10]. With NOA 65 prepolymer solution, we fabricated microneedles using a replica molding technique where the polymer was photocured (365 nm) inside a PDMS mold. The microneedle arrays have pyramidal features measuring 300 µm x 200 µm (height x width) with a tip-to-tip spacing of 500 µm

For plasmonic nanomaterial, gold nanorods (AuNRs) were synthesized in aqueous solution using the silver-assisted seed-mediated growth synthesis method with cetyltrimethylammonium bromide

stabilizing surfactant. The localized surface plasmon resonance (LSPR) of AuNRs were optimized for excitation at 785 nm in aqueous media. AuNRs were characterized by UV-visible spectroscopy, transmission electron microscopy (TEM) and scanning electron microscopy (SEM), and inductively coupled plasma optical emission spectrometry (ICP-OES). The AuNR concentation was calculated using the concentration of Au determined from ICP-OES, the dimension of AuNRs determined from TEM, and the density of Au.

Next, to fabricate plasmonic microneedle arrays, the NOA microneedle arrays were plasma treated and incubated in 1 mL solution of AuNRs (40 uL of AuNRs and 10 mM 4-MBA in 1:1 water:ethanol co-solvent) for 24 hours. After incubation, the microneedle arrays surface was rinsed with ethanol and dried with nitrogen. The schematic representation of the plasmonic microneedle arrays is shown in Figure 1.

2.2 Characterization of the plasmonic microneedle arrays

a. Optical characterization

We characterized the plasmonic microneedle arrays by taking optical and SEM images, and light extinction spectra of the sensor. Figure 2a and 2b show the dimension of the pyramidal arrays and Figure 2c and 2d show the evidence of AuNRs on the sensor surface.

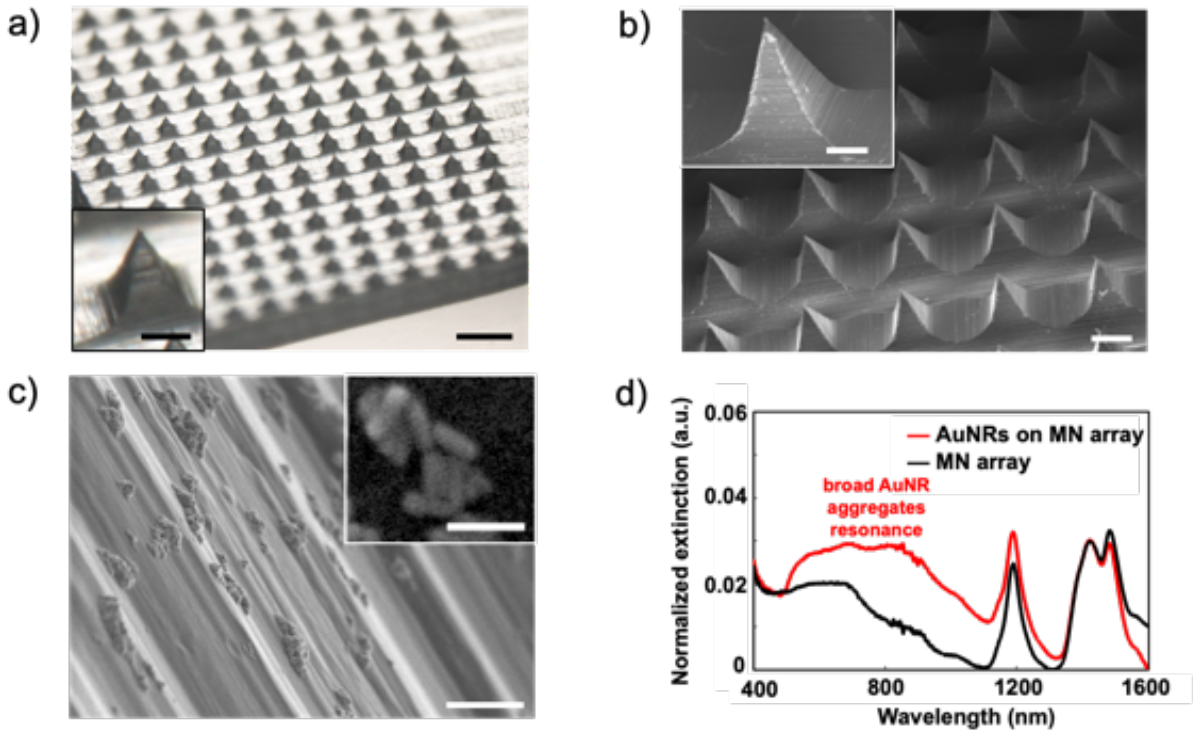

Figure 2. Optical characterization of plasmonic microneedle arrays. a) optical image of the microneedle arrays (scale bars: 500 µm and 100 µm (inset)), b) SEM image of the microneedle arrays (scale bars: 200 µm and 100 µm (inset)), c) SEM image of AuNRs on a microneedle tip

(scale bars: 1 μm and 100 nm (inset)), and d) light extinction spectra of microneedle arrays with (red) and without (black) AuNRs.

b. pH calibration curve

To demonstrate *in situ* pH sensing ability of the plasmonic microneedle arrays, we took SERS spectra of the sensor in Britton-Robinson buffer with pH ranging from 2 to 12 with 1 pH increments. As shown in Figure 3a and b, the pH-responsive peak at around 1421 cm^{-1} (carboxylate vibrational mode) shifts to 1400 cm^{-1} as the pH decreases. When calibrated, the integrated intensity of that mode is known to provide a measure for the pH of the sensor environment. We first calibrated the sensor by taking the ratio between the integrated peak intensity of the carboxylate peak (A_{cbx}) to a mode at 1076 cm^{-1} (A_{1076}), which is insensitive to pH variations. The precision was evaluated by collecting and averaging SER spectra of three replicate sensors, measuring 7 different microneedle tips for each sensor. The normalized ratio was then plotted against pH, leading to a well-known S-shaped sigmoidal curve. For comparison, we repeated the same procedure using a well-known SERS substrate, Au film-over-nanospheres (AuFON). As shown in Figure 3c, a small variation in the pK_a value of functionalized 4-MBA functionalized can be observed between the two substrates (7.13 for AuFON and 7.38 for the plasmonic microneedle arrays), which is due to the difference in the surface density of 4-MBA on the two substrates. The pK_a value for 4-MBA on AuFON was slightly lower that on the plasmonic microneedle arrays, which indicates that the density of 4-MBA is slightly higher on AuFON than on the plasmonic microneedle arrays. However, the two calibration curves in Figure 3c suggest that the two substrates are comparable.

In addition, the S-shaped calibration curves allows determination of the working pH region as the range between 5 to 9 (Figure 3c). The sensor resolution was evaluated by measuring a refined calibration curve (0.2 pH increments), which led to a nominal value of 0.23 pH units (twice the standard deviation at pH 7). Lastly, the pH reversibility of the sensor was demonstrated by cycling the pH between 2 to 12 (total of 6 cycles) shown in Figure 3e.

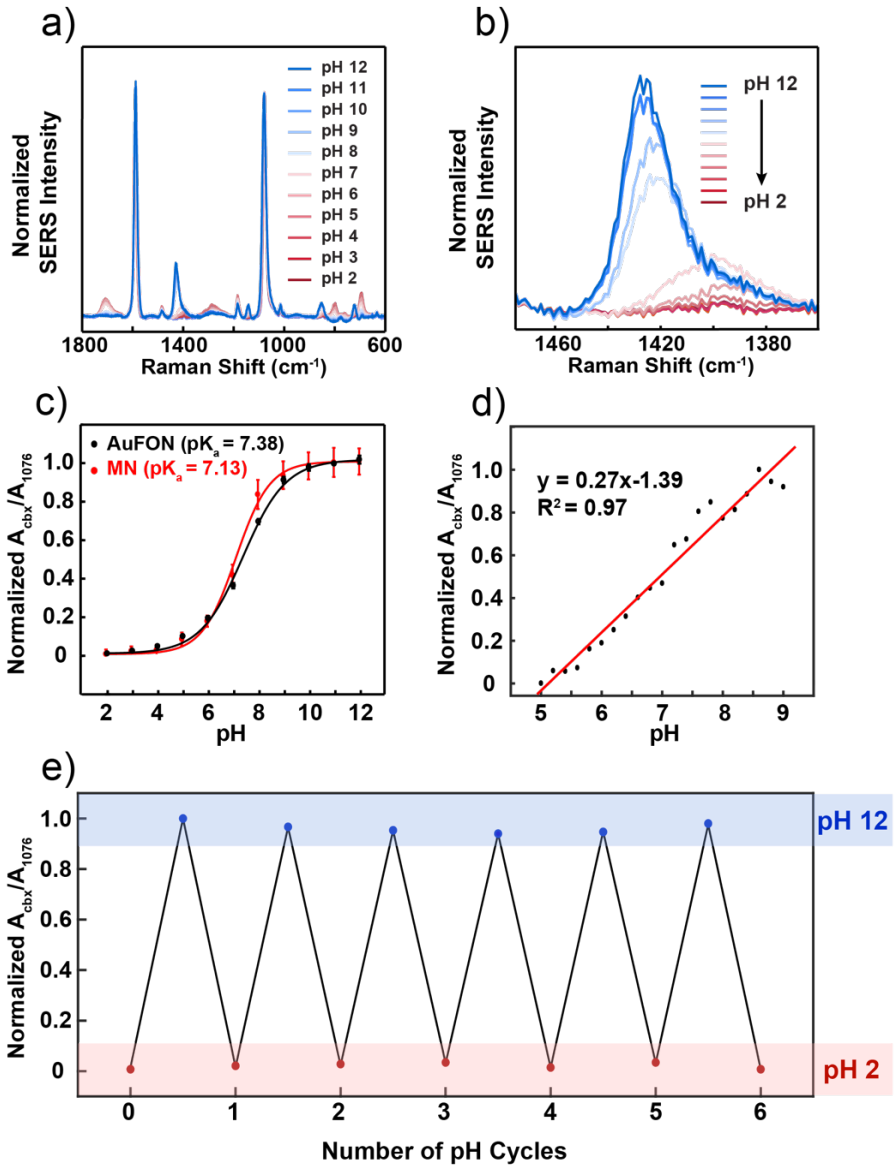

Figure 3. pH sensing with the plasmonic microneedle arrays in Britton-Robinson buffer solution. a) SERS spectra of the plasmonic microneedle arrays functionalized with 4-MBA in Britton-Robinson buffer ranging from pH 2 to 12 with pH 1 increments, and b) magnified spectra to show the pH-sensitive peak at around 1400 cm^{-1}. Each pH level is an average of 7 different microneedle tips. c) S-shaped calibration curves for the plasmonic microneedle arrays (MN) in red and a standard SERS substrate (AuFON) in black in the pH 2-12 range with 1 pH increments (MNs: 7 different tips were collected and was averaged from 3 different samples, AuFON: 5 different spots were collected from one sample and averaged). d) A linear calibration curve for the plasmonic microneedle arrays range in the pH 5-9 range with 0.2 pH increments. e) A reversibility plot for the plasmonic microneedle arrays (cycling the pH of the buffer solution between 2 to 12). The parameters for the SERS data acquisitions were λ_{ex} = 785 nm, 20x ELWD objective, t_{acq} = 1 min. The excitation power for MNs and AuFON were 1 mW and P_{ex} = 270 µW, respectively. As a note, the NOA 65 background was subtracted from all the SERS data.

2.3 *In situ* sensing in agar gel skin phantom

As an initial demonstration of *in situ* sensing, we measured the pH inside a skin phantom agar gel. First, a SER spectrum of the plasmonic microneedle arrays was acquired in air as a baseline (Figure 4a, black). Then the sensor was punctured into an agar gel skin phantom, and SER spectra were collected through the microneedle arrays while the sensor was inserted in the skin phantom (Figure 4a, blue). The carboxylate peak at around 1400 cm^{-1} shifted to 1420 cm^{-1} and the peak intensity increased when the sensor was in the skin phantom. After removing the sensor and rinsing with water, the SERS was measured again in air to check the reversibility. As shown in Figure 4a red trace, the peak at around 1420 cm^{-1} shifted back to 1400 cm^{-1}, similar to SERS spectrum taken in air before puncturing the skin phantom (Figure 4a, black). This result also demonstrates the reversibility of the sensor.

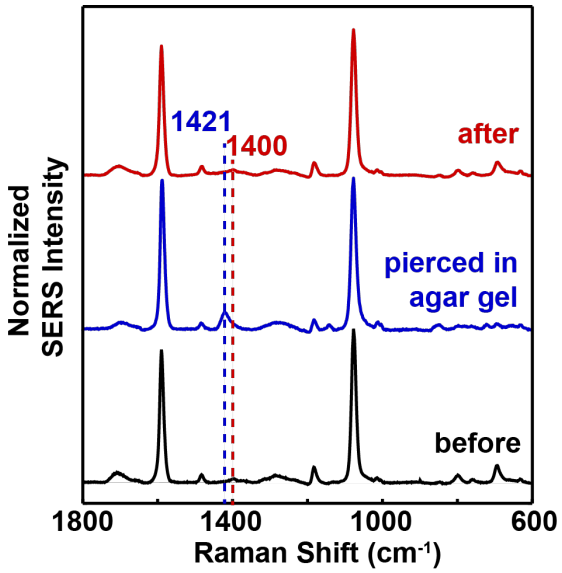

Figure 4. *In situ* sensing with plasmonic microneedle arrays in an agar gel skin phantom. SERS spectra taken in air before puncturing an agar gel (black), while pierced in agar gel (blue), and in air after puncturing an agar gel (red). Each spectrum is an average of 7 different microneedle tips. The parameters for the SERS data acquisitions were: λ_{ex} = 785 nm, 20x ELWD objective, t_{acq} = 1 min, P_{ex} = 1 mW.

2.4 Mechanical and thermal stability

Next, we tested the mechanical stability of the plasmonic microneedle arrays by comparing the SERS spectra of the sensor before and after puncturing in an agar gel skin phantom. As shown in Figure 5, no loss of 4-MBA signal was observed. To test the thermal stability of the sensor, we incubated the sensor in 1x phosphate buffered saline (PBS) solution for one month. The SER spectra before and after a month-long incubation in the buffer showed no loss of 4-MBA signal (Figure 6a). In addition, light extinction spectra of the sensor were taken over four weeks and compared to the control (MNs without AuNRs). As shown in Figure 6b, the extinction spectra show that AuNRs are present even after incubating in a buffer solution.

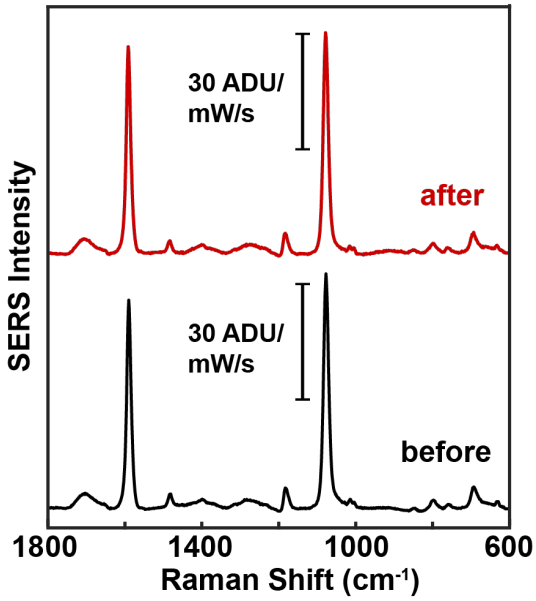

Figure 5. Mechanical stability of the plasmonic microneedle arrays. SER spectra of the sensor before and after puncturing agar gel skin phantom 10 times. Each spectrum is an average of 7 different microneedle tips. The parameters for the SERS data acquisitions were: λ_{ex} = 785 nm, 20x ELWD objective, t_{acq} = 1 min, P_{ex} = 1 mW.

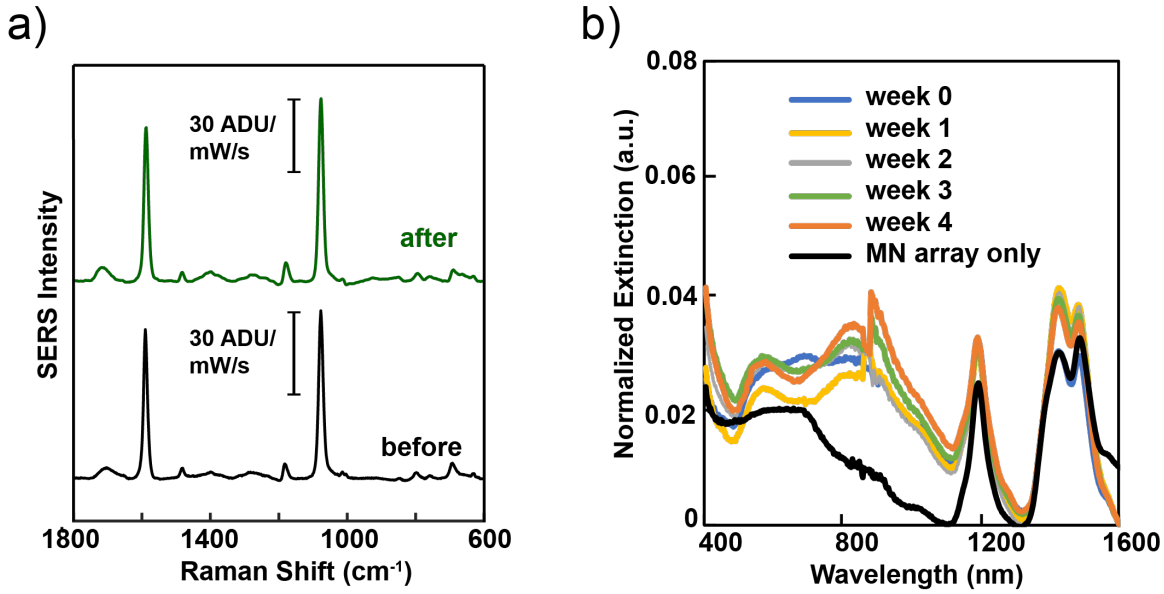

Figure 6. Thermal stability of the plasmonic microneedle arrays. SER spectra of the sensor a) before and after incubation in 1x PBS buffer for one month and b) normalized light extinction spectra of the plasmonic microneedle arrays incubated in 1 x PBS buffer over four weeks compared with a control (MN array only). Each SER spectrum is an average of 7 different microneedle tips. The parameters for the SERS data acquisitions were: λ_{ex} = 785 nm, 20x ELWD objective, t_{acq} = 1 min, P_{ex} = 1 mW.

2.5 *Ex vivo* sensing

After demonstrating *in situ* sensing in both solution and agar gel skin phantom, we proceeded to evaluate the plastform *ex vivo* sensing performance. Human skin was provided by the Skin Tissue Engineering Core Facility in Feinberg School of Medicine at Northwestern University. Optical coherence tomography (OCT) was used to image the sensor while inserted in human skin, allowing visual estimation of the penetration depth. The profile is shown in Figure 7, compared to a flat region of the sensor as a control. The images clearly demonstrate that the microneedles can be inserted in skin.

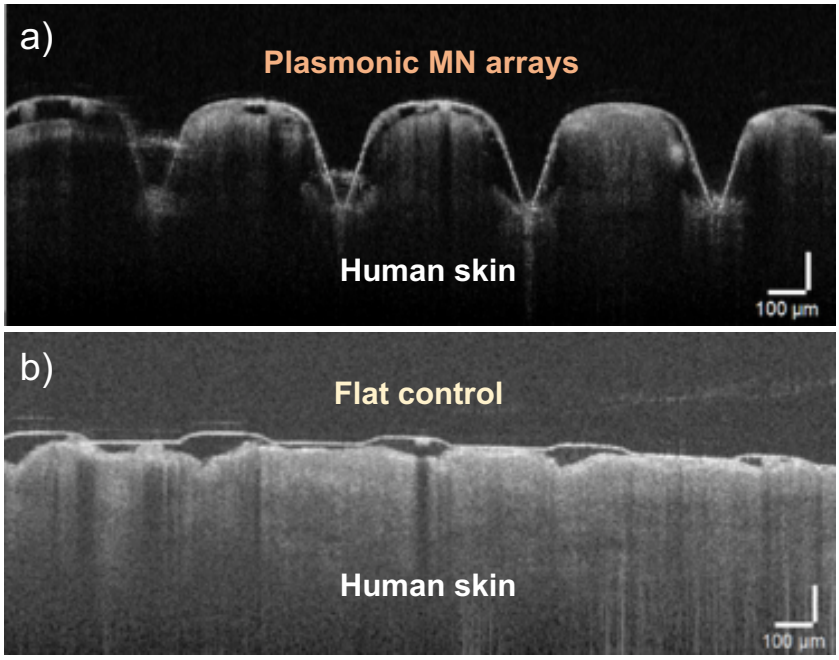

Figure 7. Optical coherence tomography (OCT) images. a) Plasmonic microneedle (MN) arrays and b) flat control (without MN) inserted onto human skin. For image acquisition, the refractive index was set to 1.524 for the cured NOA 65 (reported in the Norland Products website for NOA 65).

The sensor's ability to detect pH *in situ* in skin was evaluated next. First, the pH of human skin was modified by incubating the tissues in Dulbecco's phosphate buffered saline (DPBS) solutions with three different pHs (pH 6.6, 7.1, and 7.6) for 12 hours. The skin samples were incubated so that the dermal side was in contact with the buffer, keeping the stratum corneum side dry. After the incubation, the dermal side is carefully blotted with clean lab tissue paper. We then acquired SER spectra of the plasmonic microneedle arrays while inserted in human skin tissues with different pHs (one sensor per tissue). For controls, we took SER spectra of a plasmonic microneedle arrays in the DPBS buffer solution in which the skin was incubated. As shown in Figure 8, the A_{cbx}/A_{1076} of skin corresponds well with that of controls. We then characterized the sensor after insertion in human skin by UV-vis spectroscopy, SERS, and SEM. Light extinction spectra collected after puncturing human skin showed that AuNRs were not removed and the SERS signal was still stable (Figure 9a and b). These

conclusions were confirmed by taking SEM images of the sensor after puncturing human skin, demonstrating that the AuNRs were still intact, as shown in Figure 9c. Finally, the mechanical stability of the sensor was evaluated by applying the sensor multiple times (10 punches) to human skin. Even after multiple insertion in human skin, the SERS signal of the plasmonic microneedle arrays showed no loss of signal.

These results establish short-term stability of the sensor. However, evaluation of the long-term and in-vivo stability of the sensor are still required, as subcutaneously sensors are potentially prone to biofouling (unwanted biomaterial blocking the sensor surface), critically limiting its lifetime. We plan to investigate stability with *in vivo* studies in the following year, together with strategies to mitigate potential deleterious effects.

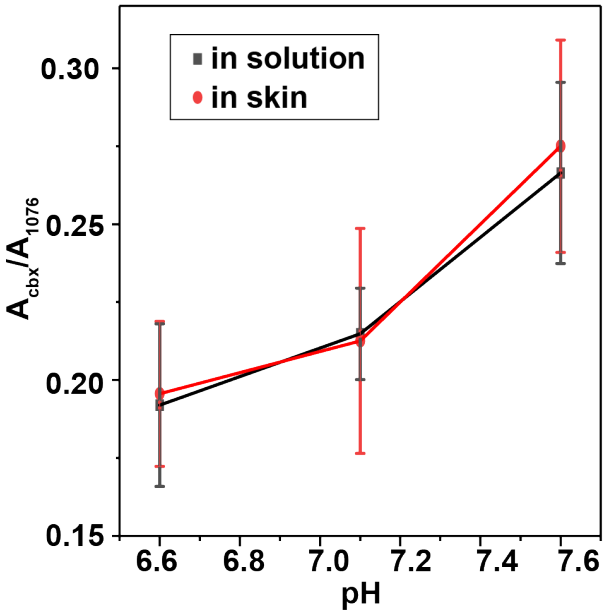

Figure 8. *Ex vivo* pH sensing with the plasmonic microneedle arrays. Plot of A_{cbx}/A_{1076} of the sensor inserted in solution (red) and placed in DPBS solution (black). SER spectra were taken at 7 different tips while focusing the laser through polymer. The parameters for the SERS data acquisitions were: λ_{ex} = 785 nm, 20x ELWD objective, t_{acq} = 1 min, P_{ex} = 1 mW.

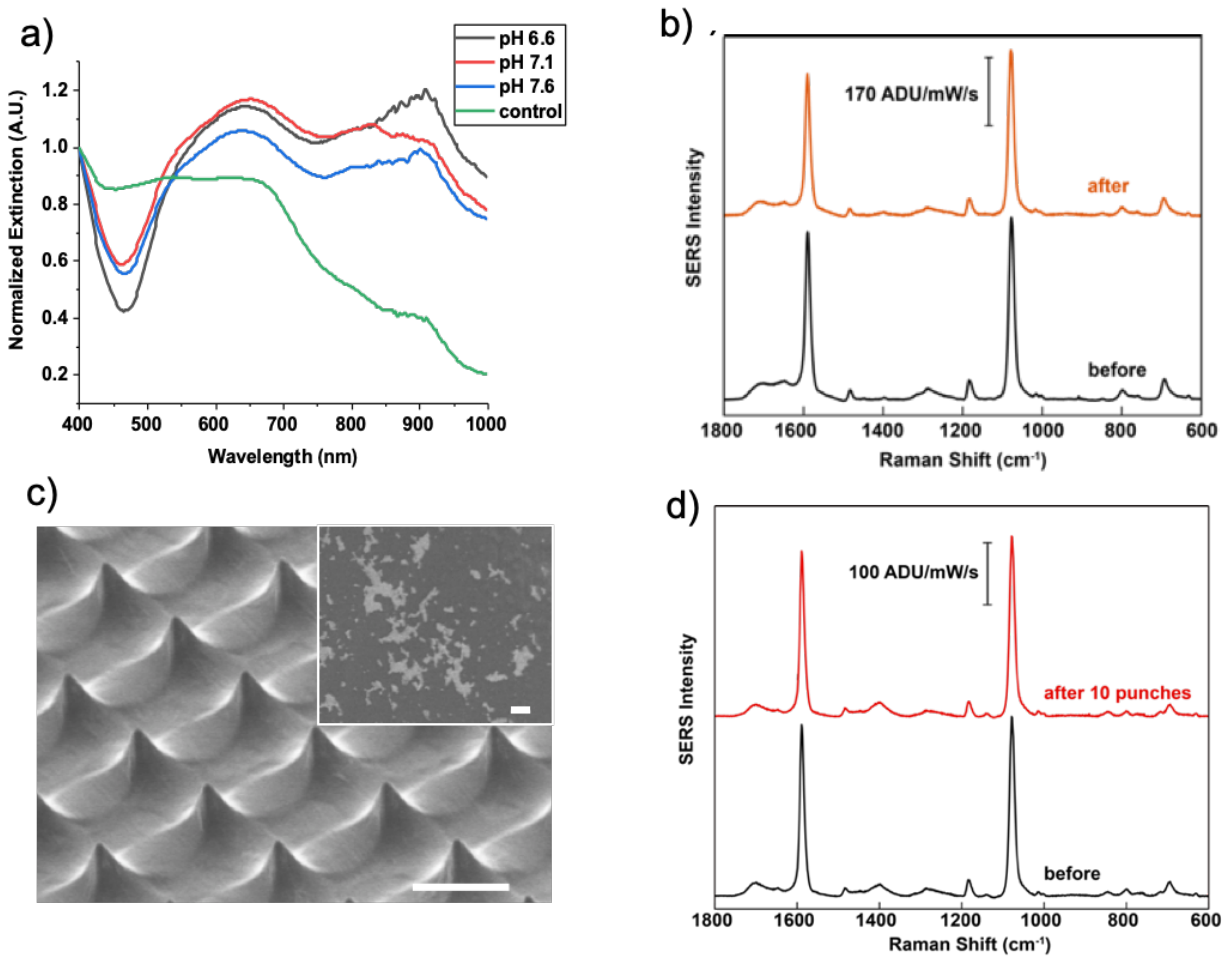

Figure 9. Characterization of the plasmonic microneedle arrays following *ex vivo* punching test. a) Normalized light extinction spectra of the sensor after insertion into human skin with pH 6.6 (black), pH 7.1 (red), pH 7.6 (blue), and without AuNRs (green) as a control. b) SER spectra of the sensor before (black) and after (orange) one time puncturing human skin (taken in air). c) SEM images of the plasmonic microneedle arrays (scale bars are 200 µm and 2 µm (inset)). d) SER spectra of the plasmonic microneedle arrays before (black) and after (red) puncturing human skin 10 times taken in pH 6.6 DPBS buffer. SERS measurements were done by focusing the laser through polymer. The parameters for the SERS data acquisitions were: λ_{ex} = 785 nm, 20x ELWD objective, t_{acq} = 1 min, P_{ex} = 1 mW.

3- Functional nanosensors

In parallel, we started investigated alternatives to deal with glucose binding affinity for the sensor. Due to the difficulties of developing a purely chemical capture agent (thoroughly described in last year report), we started exploring the possibility of using physical strategies as a parallel route to achieve analyte reversible binding onto the SERS hotspots. Encouraged by numerous reports of microneedle-based electrochemical sensors, we decided to include a coated layer of gold onto the MN

sensor, consisting of a thin Au layer. This layer is expected to allow application of potential to the surface, permitting modulation of the chemical properties of the sensor. Besides circumventing many of the challenges involved in the incorporation of chemical ligands into the sensor, the set of tools provided by Electrochemistry allows exploration of a new degree of freedom in controlling the sensor response. Indeed, preliminary/previous results from our group indicate the feasibility of using potential to modulate surface chemistry and therefore adsorption[11].

3.1 Microneedles-based EC-SERS sensor

Our first step in the development of an EC-SERS sensor was to coat an NOA microneedles (MN) patch with gold thin films of different thicknesses (40-100 nm). We realized that the hierarchical structure resulting from the molding and evaporation processes already showed inherent SERS performance, comparable to well established SERS platforms such as film-over-nanospheres (FONs). Figure 10 shows a direct comparison between FONs and Au coated microneedles, using benzenethiol (BZT) as a Raman reporter.

Preliminary tests in real human skin were also conducted and indicate the possibility of applying potential with the sensor in skin. Over the course of these initial tests, we also realized the need to apply a thin adhesion layer (5 nm) of Ti in order to avoid delamination of the gold coating. After we started using a Ti adhesion layer, no evident delamination of the sensor was observed.

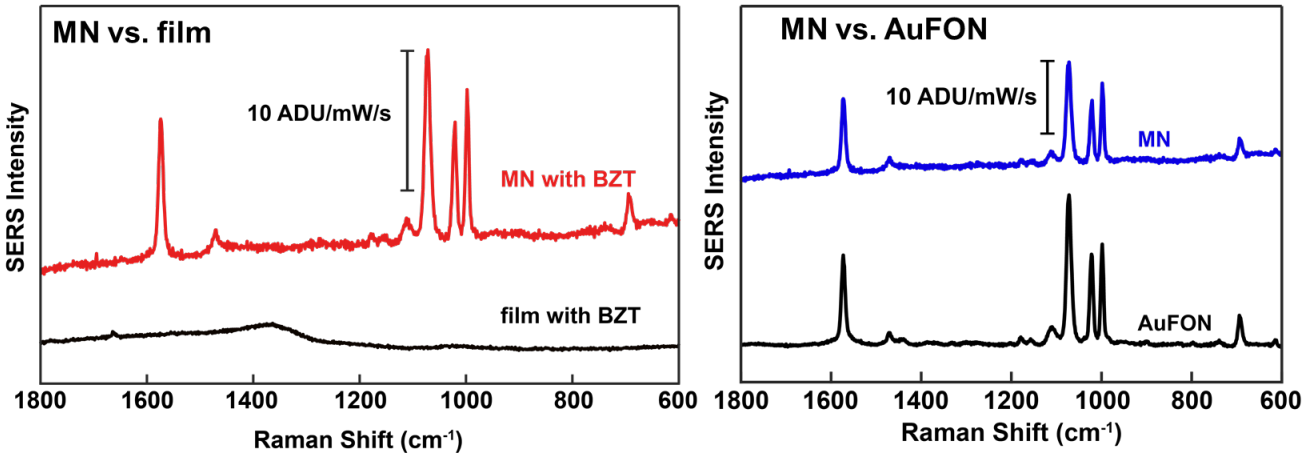

Figure 10. Evaluation of the SERS performance of the EC-SERS-MN (a) the SERS enhancement of Au-MN is compared with a flat film over NOA, using benzenethiol as a Raman reporter (b) Comparison of Au-MN SERS enhancement with a well stablished SERS-substrate (Au-FON), showing comparable performances. For all spectra λ_{ex} = 785 nm, 20x ELWD objective, t_{acq} = 1 min, P_{ex} = 1 mW.

Next, we proceeded to analyze the effect of electrochemical potential on the SERS response, using the setup indicated in Figure 11. Owing to glucose's low Raman scattering cross-section, we conducted our initial tests in the presence of 1 mM caffeine, a model molecule relevant to biosensing,

in the presence of 100mM phosphate buffer (pH 7.4).

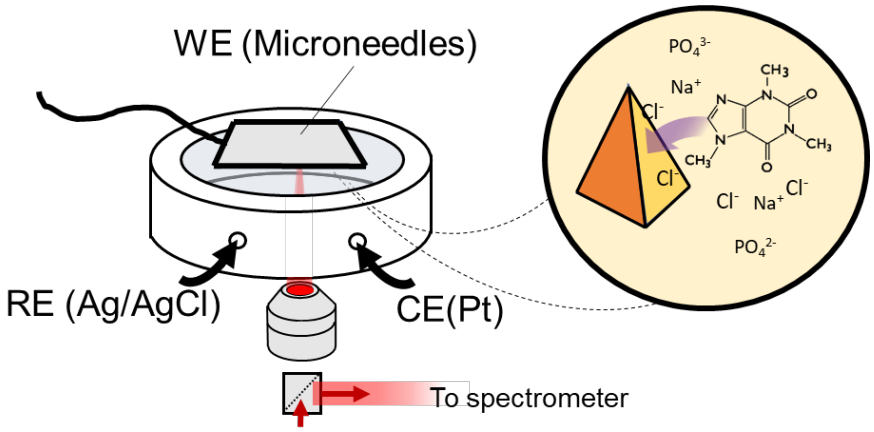

Figure 11. Schematics of the electrochemical SERS setup and experiment concept

The results, shown in Figure 12, indeed indicate that cycling the potential (E) between -0.8 and 1 V (vs Ag/AgCl) generates drastic spectral changes, corresponding to different adsorption and redox events. Initially, at E close to open circuit potential (OCP), only a faint band can be observed, near 250cm^{-1}, (black trace in Figure 12) which corresponds to electrolyte adsorption on Au surface (Au-Cl) [12]. As the potential is raised, the intensity of this band increases, until E~0.7V where Au oxide forms, which can be observed through the appearance of a broad band at ~550 cm^{-1}, which attenuates all other Raman bands. When the potential is brought to lower potentials, however, caffeine characteristic bands clearly appear, such as the 555 cm^{-1} peak, associated to a perturbated pyrimidine ring breathing mode, and 1325 cm^{-1}, related to imidazole trigonal ring stretching, among others. At more cathodic potentials, these peaks disappear again, only to reappear during the following cycle. A representative cycle is shown in detail on Figure 12.

This experiment demonstrates the potential of electrochemistry to reversibly modulate surface chemistry, and therefore SERS response of the biosensor.

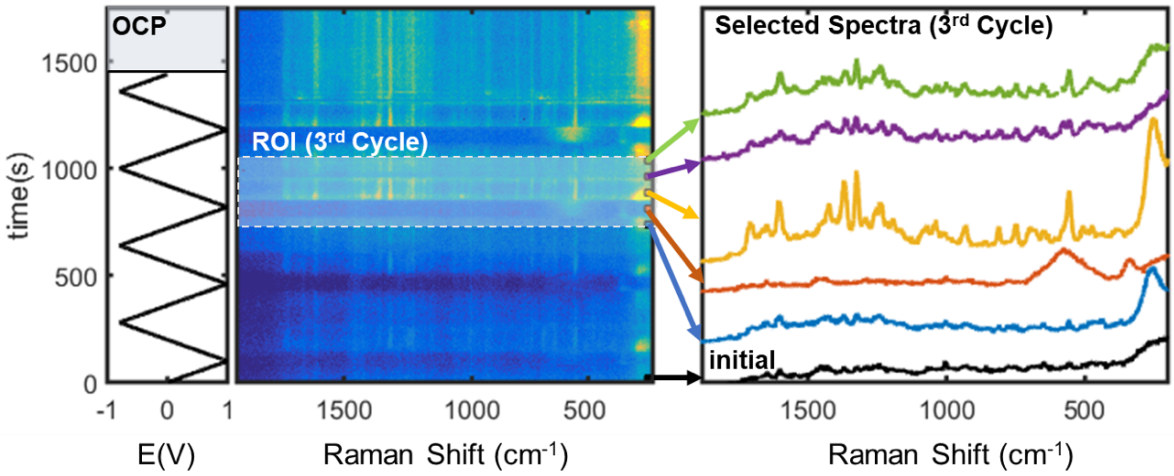

Figure 12. Electrochemical variation Evaluation of the SERS performance of the EC-SERS-MN (a) Schematics indicating the setup used for the electrochemical experiments (b) Temporal evolution of the SERS response as a function of potential. Selected spectra are shown, corresponding to a representative cycle.

3.2 Incorporating principle component analysis (PCA)

The ability to modulate adsorption also allowed the application of multivariate methods which are sensitive to the signal variance, such as Principal Component Analysis (PCA). PCA is a popular dimensionality reduction technique which decomposes a set of correlated variables into a lower-dimensional linear representation, preserving the dataset most dominant dynamics. In short, the data is described in terms of the eigenvectors of the dataset correlation matrix. In other words, it discovers new representations of the data by considering a linear combination of variables which maximize the independence of each component (i.e. minimize the redundancy). In the general case the different variables can be very different, making their combination essentially uninterpretable (i.e. comparing apples and oranges). For a spectrum, an ensemble of N different single wavenumber measurements (one for every pixel of the detector), the variables are all comparable, which allows the eigenvectors to be seen as spectra on their own and therefore reasonably interpreted.

These methods traditionally are quite sensitive to sample-to-sample variations, requiring extensive preprocessing of the data in order to extract interpretable physical-chemical information. In our case, however, the data matrix used to extract the spectra representations, is evaluated locally (e.g. at a given spot and sample), which minimizes background influence and other parasitic phenomena. Indeed, the PCA algorithm is applied to data with minimal amounts of preprocessing (only cosmic rays are removed), which makes the methodology more appealing to practical applications and less prone to artifacts due to biased preprocessing.

Figure 13 below shows the decomposition in principal components of the data collected in the experiment shown in Figure 12. In the left figure, the eigenvectors (also called the scores) are shown,

which can be readily interpreted in terms of chemical species. Indeed, the 2nd Principal Component (PC) eigenvector reveals spectra closely related to Au-Cl vibration (250 cm^{-1} peak), while the 3rd is dominated by the Au- oxide broad band ($\sim 550\ cm^{-1}$) and the 4th contain all caffeine relevant peaks, indicated by the gray lines in the figure. Together with the 1st PC, which is essentially featureless, these PC account for 95% of the dataset dynamics.

Plotting the time evolution of the loadings of each PC as a function of time is also interesting, as it allows to show the temporal evolution of the contribution of each chemical species to the total spectrum. The curves, shown in the right panel of Figure 13, indeed reproduce the trends empirically observed, e.g. the increase of Au-Cl vibration with potential, followed by appearance of Au-oxide and later appearance of caffeine peaks.

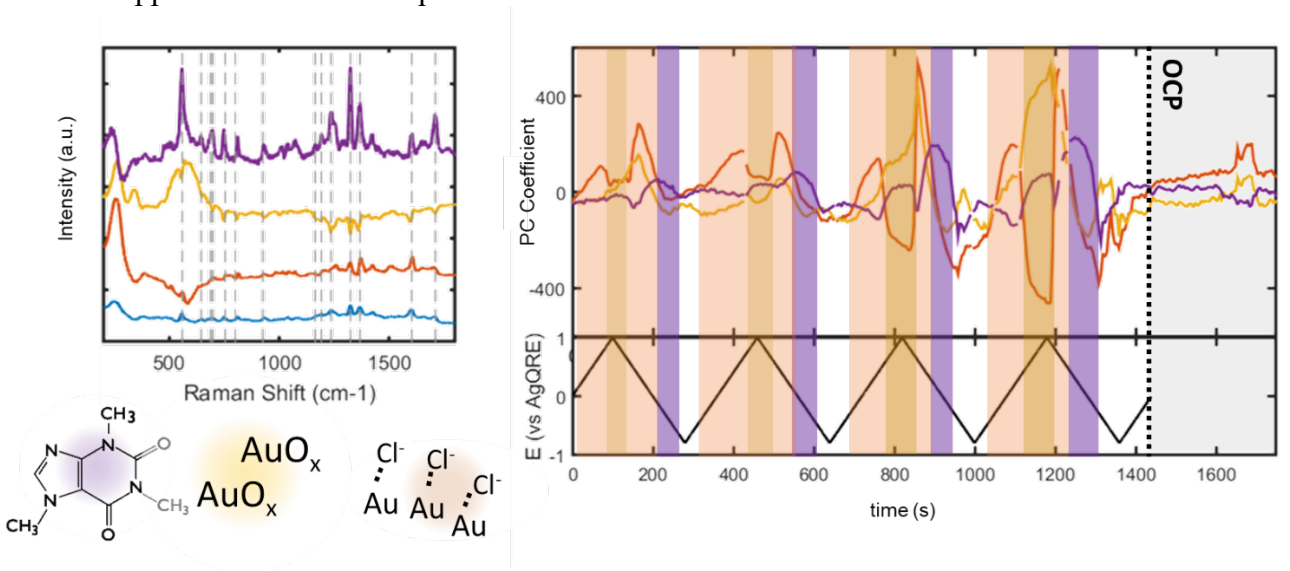

Figure 13. Principal component Analysis of the caffeine experiment. The eigenvectors of the data matrix can be interpreted spectrally.

In order to better understand the separation processes, we applied PCA to random subsamples of the data, which led to similar results, but with an increased degree of spectral crosstalk between the different eigenvectors. Besides demonstrating the robustness of the method, this suggests that the separation power indeed stems from the ability to perform numerous adsorb/desorb cycles, increasing the correlation between pixels belonging to the same spectrum, which can be captured by the algorithm.

3.3 Separating Mixtures using EC-SERS PCA.

The results demonstrate the ability of spectro-electrochemical experiments in conjunction with PCA to scrutinize between chemical phenomena with different dynamics (adsorption of molecules with different chemical properties, substrate redox reaction, etc.). Next, we demonstrate that the same strategy can also be used to separate molecules with similar chemical structure. In order to test that idea, we introduced 1 mM of theobromine in addition to the 1mM caffeine and 100 mM phosphate buffer solution. Theobromine and caffeine have similar chemical structure, only differing by a methyl

group, which might suggest similar adsorption behavior. The potential was again cycled between -0.8 and 1V. The eigenvectors extracted from the data after 10 cycles are shown in Figure 14. For simplicity, the spectral region of interest was limited to $\nu > 400\ cm^{-1}$. As before, the 2nd PC contains the broad feature associated with Au oxide at $\sim 550 cm^{-1}$ (orange trace). The 3rd PC (shown in yellow) contains all peaks relative to Theobromine (dashed vertical lines), while the 4th (in purple) contains caffeine related vibration bands. These results demonstrate that even closely related structures can be separated through potential modulation and multivariate analysis. This ability is likely to be an asset in a real *in vivo* biosensor design, helping to cope with different chemical interference phenomena, including bio-fouling, which are expected to perturb the medium to long-term performance of the sensor.

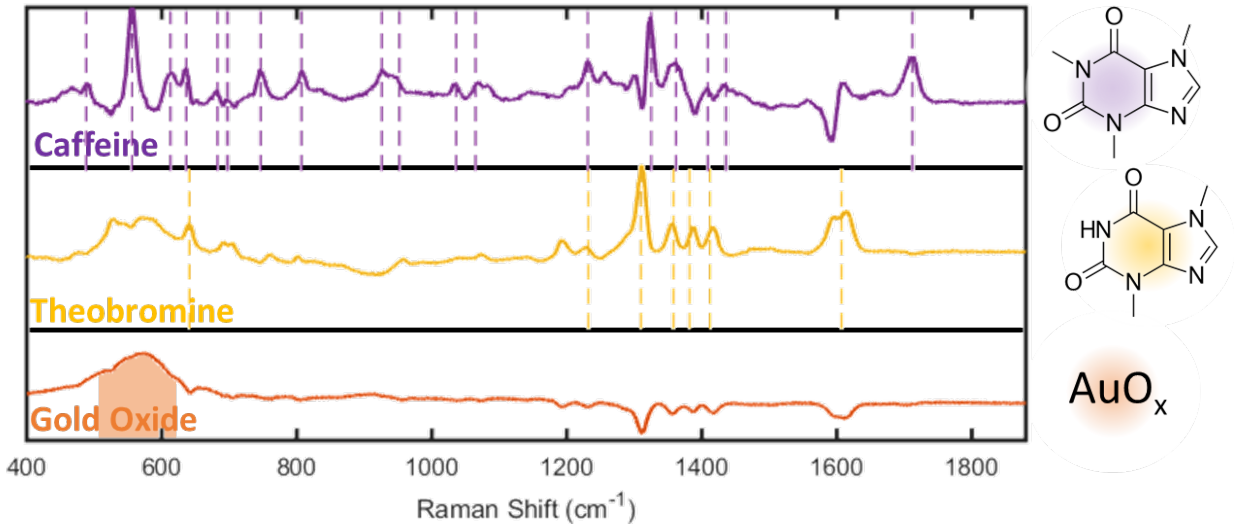

Figure 14. Separation of similar molecules by PCA of EC-SERS experiments. Eigenvectors extracted from a total of 700 spectra, $t \sim 3500\ s$. One can clearly identify the presence of caffeine peaks on the 4th PC (top), while the 3rd shows theobromine vibration bands (middle), and the 2nd primarily contains the broad mode associated with gold oxide, albeit with a parasitic presence of theobromine bands due to correlation between theobromine adsorption and oxide presence.

References:

(1) Ribet, F.; Stemme, G.; Roxhed, N. Real-Time Intradermal Continuous Glucose Monitoring Using a Minimally Invasive Microneedle-Based System. *Biomed Microdevices*. **2018**, *20*, 101.

(2) Miller, P. R.; Skoog, S. A.; Edwards, T. L.; Lopez, D. M.; Wheeler, D. R.; Arango, D. C.; Xiao, X.; Brozik, S. M.; Wang, J.; Polsky, R.; Narayan, R. J. Multiplexed Microneedle-Based Biosensor Array for Characterization of Metabolic Acidosis. *Talanta* **2012**, *88*, 739–742.

(3) Bollella, P.; Sharma, S.; Cass, A. E. G.; Antiochia, R. Microneedle-Based Biosensor for Minimally-Invasive Lactate Detection. *Biosens. Bioelectron.* **2019**, *123*, 152–159.

(4) Windmiller, J. R.; Valdés-Ramírez, G.; Zhou, N.; Zhou, M.; Miller, P. R.; Jin, C.; Brozik,

S. M.; Polsky, R.; Katz, E.; Narayan, R.; et al. Bicomponent Microneedle Array Biosensor for Minimally-Invasive Glutamate Monitoring. *Electroanalysis* **2011**, *23* (10), 2302–2309.
(5) Mishra, R. K.; Vinu Mohan, A. M.; Soto, F.; Chrostowski, R.; Wang, J. A Microneedle Biosensor for Minimally-Invasive Transdermal Detection of Nerve Agents. *Analyst* **2017**, *142* (6), 918–924.
(6) Mohan, A. M. V.; Windmiller, J. R.; Mishra, R. K.; Wang, J. Continuous Minimally-Invasive Alcohol Monitoring Using Microneedle Sensor Arrays. *Biosens. Bioelectron.* **2017**, *91*, 574–579.
(7) Liliensiek, S. J.; Wood, J. A.; Yong, J.; Auerbach, R.; Nealey, P. F.; Murphy, C. J. Modulation of Human Vascular Endothelial Cell Behaviors by Nanotopographic Cues. *Biomaterials* **2010**, *31* (20), 5418–5426.
(8) Meng, J.; Kong, H.; Han, Z.; Wang, C.; Zhu, G.; Xie, S.; Xu, H. Enhancement of Nanofibrous Scaffold of Multiwalled Carbon Nanotubes/Polyurethane Composite to the Fibroblasts Growth and Biosynthesis. *J. Biomed. Mater. Res. - Part A* **2009**, *88* (1), 105–116.
(9) Sollier, E.; Murray, C.; Maoddi, P.; Di Carlo, D. Rapid Prototyping Polymers for Microfluidic Devices and High Pressure Injections. *Lab Chip* **2011**, *11* (22), 3752–3765.
(10) Mohr, J. C.; de Pablo, J. J.; Palecek, S. P. 3-D Microwell Culture of Human Embryonic Stem Cells. *Biomaterials* **2006**, *27* (36), 6032–6042.
(11) Zaleski, S.; Clark, K. A.; Smith, M. M.; Eilert, J. Y.; Doty, M.; Van Duyne, R. P. Identification and Quantification of Intravenous Therapy Drugs Using Normal Raman Spectroscopy and Electrochemical Surface-Enhanced Raman Spectroscopy. *Anal. Chem.* **2017**, 89, 2497-2504.
(12) Chan, M. Y.; Leng, W.; Vikesland, P. J.; Surface-Enhanced Raman Spectroscopy Characterization of Salt-Induced Aggregation of Gold Nanoparticles *ChemPhysChem* **2018**, 19, 24-28.
(13) Pavel, I; Szeghalmi, A.; Moigno, D.; Cinta, S.; Kiefer, W. Theoretical and pH Dependent Surface enhanced Raman Spectroscopy Study on Caffeine *Biopolymers* **2003**, 72, 25-37.

Opportunities for training and professional development provided by the project

Dr. Vitor Brasiliense joined the project in July 2018 and worked together with Ji Eun Park to develop EC-SERS microneedle platform. Dr. Ju-Young Kim joined the group in June of 2019 and she is now fully trained on a laser table and instruments from core facilities (SEM and AFM).

Dissemination of results to communities of interest

Ji Eun Park and Vitor Brasiliense took part in the 'All Scout Nanoday' outreach event organized by the International Institute for Nanotechnology and hosted in part by the Van Duyne lab. They engaged with a young audience (~10-14 year old girl and boy scouts from the Chicago area) to communicate about nanotechnology research and careers in science.

Plan for the next reporting period towards accomplishing outlined goals

Up to this point we have a robust microneedle biosensing platform which is robust and capable of providing long term continuous monitoring of *in vivo* chemical properties, such as pH (section 2). Furthermore, we have identified a physical strategy which might help deal with chemical interference from a complex medium such as in *in vivo* measurements. Having understood how electrochemical methods can be used to mitigate analyte low binding affinity for the substrate (section 3), we are currently working in applying these ideas to detection of glucose. Preliminary results using Au FONs indeed indicate that EC potential could be the key to detecting glucose binding, shown in Figure 15, obtained after cycling the Au surface in 1 mM glucose solution in the presence of 50 mM KCl. It suggests that glucose molecules can be directly detected in solution.

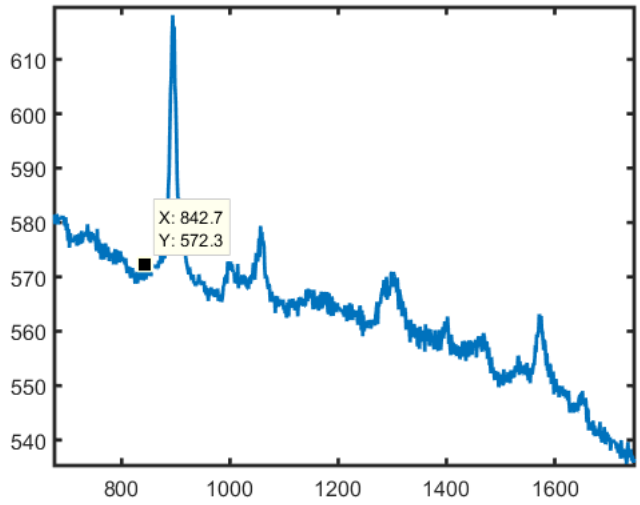

Figure 15. SER spectrum of Au microneedles in 1 mM glucose solution with 50 mM KCl.

Our planned next step is to combine the potential manipulation capability of the EC-SERS MN sensor with the high enhancement provided by plasmonic objects (such as nanoparticles) by incorporating plasmonic nanoparticles to the EC-SERS microneedle arrays sensor. We expect this combined approach to allow easier detection of analytes with a small Raman cross-section, such as glucose. While testing our sensors in skin (*ex vivo*), we are also currently initiating a collaboration with a core facility that will allow *in vivo* experiments to be conducted, using the SESORS developed setup (section 1).

In parallel, we are developing anti-biofouling strategies using Gantrez-PEG polymer as a semipermeable selective membrane. We expect to apply such a layer onto the sensor surface as shown in Figure 16, extending the sensor long-term stability by preventing biological interference and nanoparticles desorption from the sensor surface.

Over this year, we plan to converge all the functional aspects developed in this year into a single microneedle sensor, achieving a biosensor which can deal with the challenges of continuous transdermal monitoring of glucose.

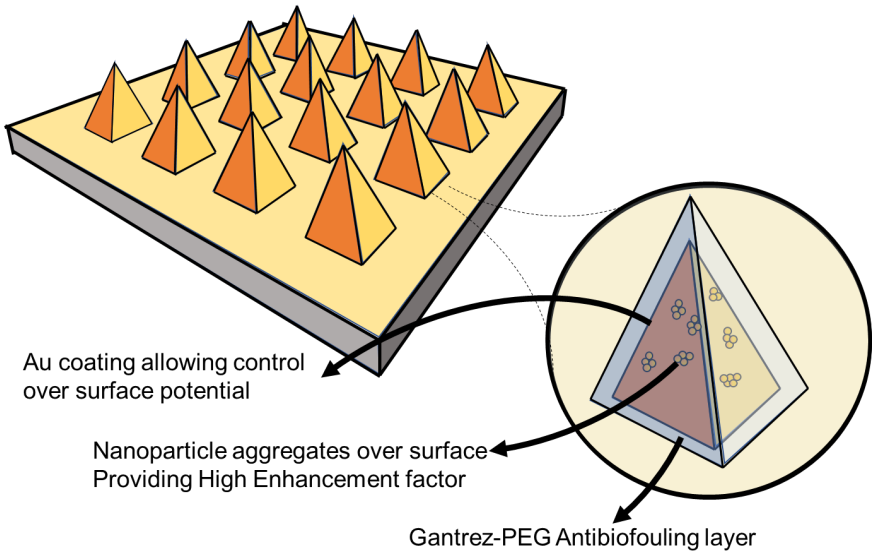

Figure 16. Design of an EC-SERS microneedle arrays sensor with a Gantrez-PEG antibiofouling layer.

4. IMPACT

Impact on the development of the principal discipline(s) of the project

We have developed a plasmonic microneedle arrays sensor and successfully applied the sensor in skin tissues (e.g., human, rat, pig). To evaluate the platform capability, we have demonstrated its use for pH sensing. This work has been accepted for publication in a high impact journal (Nano Letters). While investigating alternatives to chemical capture ligands, we have identified a general strategy to reversibly bind analytes to our sensor surface using potential. This is a general concept which is likely to be applied to a wide range of biosensors. In the context of spectro-electrochemical biosensors, we have identified and demonstrated a strategy that allows interpretable multivariate analysis to be deployed. We expect these results to be of interest to the general biosensing community as it introduces a flexible tool that can be applied in various different contexts/sensors. We're currently working on a manuscript which will be submitted for publication this year, which will cover the results shown in section 3 of this report.

Impact on other disciplines

Nothing to report.

Impact on technology transfer

Nothing to report yet.

Impact on society beyond science and technology

Nothing to report.

5. CHANGES/PROBLEMS

Changes in approach and reasons for change

Nothing to report.

Actual or anticipated problems or delays and actions or plans to resolve them
We encountered difficulty in detecting glucose using capture ligands (with boronic acid functional group) after surface functionalization. However, we recently developed a strategy to detect analytes of interest by applying potential to a SERS active sensor surface. Using this method, we successfully detected biomolecules, such as caffeine and theobromine. Next, we plan to detect glucose using this strategy (without using a capture ligand).

In addition, we plan to perform *in vivo* study using the plasmonic microneedle arrays in collaboration with the Developmental Therapeutics Core at Northwestern University.

Changes that had a significant impact on expenditures

Nothing to report.

Significant changes in use or care of human subjects, vertebrate animals, biohazards, and/or select agents

Nothing to report.

6. PRODUCTS

Publications, conference papers, and presentations

- **Journal publications**
  1. Park, J.; Yonet-Tanyeri, N.; Vander Ende, E.; Henry, A. I.; Perez White, B. E.; Mrksich, M.; Van Duyne, R. P. Plasmonic Microneedle Arrays for in Situ Sensing with Surface-Enhanced Raman Spectroscopy (SERS) *Nano Letters,* **2019***, 19,* 6862-6868.

  2. Brasiliense, V.; Park, J.; Van Duyne, R. P.; Mrksich, M. (2019) Electrochemical Microneedles as Receptor-free Plasmonic Biosensors: Spectral Separation through Local Representations and Potential Modulation (in preparation).

- **Books or other non-periodical, one-time publications**

Nothing to report.

- **Other publications, conference papers, and presentations**

- Dr. Nihan Yonet-Tanyeri presented her work with a poster presentation on the Society for Biomaterials (SFB) Biomaterials Day at the University of Michigan-Ann Arbor, MA in October 2017 entitled "SERS Based Transdermal Patches for Nanosensing."

- Dr. Nihan Yonet-Tanyeri was also invited to give an oral presentation at the Annual Meeting of American Institute of Chemical Engineers (AIChE, October 28 - November 2, 2018) that will be held in Pittsburgh, PA. Her talk is entitled "Non-invasive Plasmonic Biosensors for In Situ Glucose Monitoring."

- Ji Eun Park presented her work with a poster presentation at American Chemistry Society National Meeting and Expo at Orlando, Florida in April 2019 entitled "Plasmonic Microneedles for Continuous pH Monitoring Using Surface-Enhanced Raman Spectroscopy."

- **Website(s) or other Internet site(s)**

  A brief description of the SERS-enabled biosensing efforts in the Van Duyne lab is provided on the group webpage:
  http://sites.northwestern.edu/vanduyne/research/sers-biosensing/

  Direct access to previously cited publications is also provided on the website:
  http://sites.northwestern.edu/vanduyne/publications/

- **Technologies or techniques**

  Plasmonic microneedles described in Accomplishments are technologies directly resulting from this program.

- **Inventions, patent applications, and/or licenses**

  Nothing to report.

- **Other Products**

  Nothing to report.

7. PARTICIPANTS AND OTHER COLLABORATING ORGANIZATIONS

- **Individuals working on the project**

Name:	*Richard Van Duyne (deceased, July 2019)*
Name:	*Milan Mrksich (no change)*

Name:	*Ji Eun Park (no change)*
Name:	*Emma Vander Ende (left in May 2019)*
Name:	*Eric Berns (no change)*
Name:	*Tsatsral Iderzorig (left in Feb 2019)*
Name:	*Pradeep Bugga (left in Feb 2019)*

Name:	*Vitor Brasiliense*
Project Role:	*Postdoctoral Fellow*
Researcher Identifier (e. ORCID ID):	*N/A*
Nearest person mon worked:	*12*
Contribution to Project:	*Dr. Brasiliense has performed work on th electrochemistry and multivariate analysis*
Funding Support:	*N/A*

Name:	*Ju-Young Kim*
Project Role:	*Postdoctoral Fellow*
Researcher Identifier (e. ORCID ID):	*N/A*
Nearest person mon worked:	*6*
Contribution to Project:	*Dr. Kim has performed work on fabricating hydroge based microneedles*
Funding Support:	*N/A*

- **Change in the active other support of the PD/PI(s) or senior/key personnel since the last reporting period.**

  Nothing to report.

- **Other organization involved as partners**

  Organization Name: NU*ANCE*, Northwestern University
  Location of Organization: Evanston, IL
  Partner's contribution to the project: Facilities; project staff from the Van Duyne lab and Mrksich lab used Northwestern's electron microscopy facility to characterize the morphology of the microneedle platforms by scanning electron microscopy.

  Organization Name: Skin Tissue Engineering Core, Northwestern University
  Location of Organization: Chicago, IL
  Partner's contribution to the project: project staff from the Van Duyne lab and Mrksich lab collaborated with the core staff for skin experiments.

8. SPECIAL REPORTING REQUIREMENTS

   Since this is a collaborative award and the PI (Richard Van Duyne) deceased, the Partnering PI (Milan Mrksich) will submit one report.

9. APPENDICES

   None.